Hindawi Publishing Corporation
International Journal of Navigation and Observation
Volume 2008, Article ID 651437, 8 pages
doi:10.1155/2008/651437

Research Article

Joint L-/C-Band Code and Carrier Phase Linear Combinations for Galileo

Patrick Henkel[1] and Christoph Günther[1, 2]

[1] *Institute of Communications and Navigation, Technische Universität München (TUM), Theresienstraße 90, 80333 München, Germany*
[2] *German Aerospace Center (DLR), Institute of Communications and Navigation (IKN), Münchner Straße 20, 82234 Weßling/Oberpfaffenhofen, Germany*

Correspondence should be addressed to Patrick Henkel, patrick.henkel@tum.de

Received 1 August 2007; Revised 27 November 2007; Accepted 15 January 2008

Recommended by Gerard Lachapelle

Linear code combinations have been considered for suppressing the ionospheric error. In the L-band, this leads to an increased noise floor. In a combined L- and C-band (5010–5030 MHz) approach, the ionosphere can be eliminated and the noise floor reduced at the same time. Furthermore, combinations that involve both code- and carrier-phase measurements are considered. A new L-band code-carrier combination with a wavelength of 3.215 meters and a noise level of 3.92 centimeters is found. The double difference integer ambiguities of this combination can be resolved by extending the system of equations with an ionosphere-free L-/C-band code combination. The probability of wrong fixing is reduced by several orders of magnitude when C-band measurements are included. Carrier smoothing can be used to further reduce the residual variance of the solution. The standard deviation is reduced by a factor 7.7 if C-band measurements are taken into account. These initial findings suggest that the combined use of L- and C-band measurements, as well as the combined code and phase processing are an attractive option for precise positioning.

1. INTRODUCTION

The integer ambiguity resolution of carrier-phase measurements has been simplified by the consideration of linear combinations of measurements at multiple frequencies. Early methods were the three-carrier ambiguity resolution (TCAR) method introduced by Forssell et al. [1], as well as the cascade integer resolution (CIR) developed by Jung et al. [2].The weighting coefficients of three-frequency phase combinations are designed either to eliminate the ionosphere at the price of a rather small wavelength or to reduce the ionosphere only by a certain amount with the advantage of a larger wavelength.

The systematic search of all possible GPS L1-L2 widelane combinations has been performed by Cocard and Geiger [3]. The L1-L2 linear combination of maximum wavelength (14.65 m) amplifies the ionospheric error by a factor 350. Collins gives an overview of reduced ionosphere L1-L2 combinations with wavelengths up to 86.2 cm $(+1, -1$ widelane) in [4].

The authors have extended this work to three-frequency (3F) Galileo combinations (E1-E5a-E5b) in [5]. A 3F widelane combination with a wavelength of 3.256 m and an ionospheric suppression of 16.4 dB was found. Furthermore, a 3F narrowlane combination with a wavelength of 5.43 cm could reduce the ionospheric error by as much as 36.7 dB. Sets of linear carrier-phase combinations that are robust against residual biases were studied in [6]. The integer ambiguities of the linear combinations can be estimated by the least-squares ambiguity decorrelation adjustment (LAMBDA) algorithm developed by Teunissen [7]. The method includes an integer transformation which can also be used to determine optimum sets of linear combinations [8].

In this paper, the authors used code- and carrier-phase measurements in the linear combinations for obtaining ionospheric elimination, large wavelengths, and a low noise level at the same time. The E5a and E5b code measurements are of special interest due to their large bandwidth (20 MHz) and their low associated Cramer-Rao bound of 5 cm [9]. The C-band phase measurements are particularly interesting due

to their small wavelength and their thus reduced phase noise. The properties of code-carrier linear combinations are optimized by including both L- and C-band measurements. The cost function is defined as the ratio of half the wavelength and the noise level of the ionosphere-free code-carrier combination. It is called combination discrimination and it is a measure of the radius of the decision regions expressed in units given by the standard deviation of the noise. The L-Band signals of Galileo are defined in the Galileo-ICD [10]. The C-band signals are foreseen in a band between 5010 MHz to 5030 MHz [11]. The signal propagation and tracking characteristics in the C-band have been analyzed by Irsigler et al. [12]. The larger frequencies result in an additional free space loss of 10 dB that has to be compensated by a larger transmit power.

The paper is organized as follows: the next section introduces the design of code-carrier linear combinations. The underlying trade-off between a low noise level and strong ionospheric reduction turns out to be controlled by the weighting coefficients of E5a/E5b code measurements.

In Section 3, code-carrier linear combinations are computed in a way that include both L- and C-band measurements. An ionosphere-free code-only combination is determined that benefits from a 4.5 times lower noise level than a pure L-band combination. Furthermore, a pure L-band ionosphere-free code-carrier combination with a wavelength of 3.215 m and a noise standard deviation of 3.9 cm is found. The combined use of the two reduces the probability of wrong fixing of the latter solution by 9 orders of magnitude with respect to a pure L-band solution.

The use of C-band measurements for ionosphere-free carrier smoothing is discussed in Section 4: an ionosphere-free code-carrier combination of arbitrary wavelength is smoothed by a pure phase combination. The low noise level of C-band measurements provides a linear combination that benefits from an 8.9 dB lower noise level as compared to the equivalent L-band combination.

2. CODE-CARRIER LINEAR COMBINATIONS

Linear combinations of carrier-phase measurements are constructed to increase the wavelength (widelane), suppress the ionospheric error, and to simplify the integer ambiguity resolution. The properties of the linear combinations can be improved by including weighted code measurements into the pure phase combinations. Figure 1 shows a three frequency (3F) linear combination where the phase measurements are weighted by α, β, γ, and the code measurements are scaled by a, b, c. The weighting coefficients are generally restricted by a few conditions: first, the geometry should be preserved, that is

$$\alpha + \beta + \gamma + a + b + c \stackrel{!}{=} 1. \tag{1}$$

Moreover, the superposition of ambiguities should be an integer multiple of a common wavelength λ, that is

$$\alpha\lambda_1 N_1 + \beta\lambda_2 N_2 + \gamma\lambda_3 N_3 \stackrel{!}{=} \lambda N, \tag{2}$$

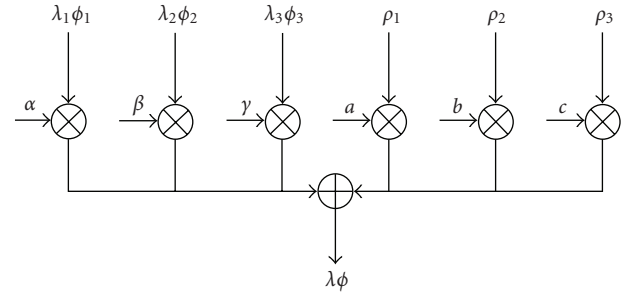

Figure 1: Linear combination of carrier-phase and code measurements.

which can be split into three sufficient conditions

$$i = \frac{\alpha\lambda_1}{\lambda} \in \mathbb{Z}, \qquad j = \frac{\beta\lambda_2}{\lambda} \in \mathbb{Z}, \qquad k = \frac{\gamma\lambda_3}{\lambda} \in \mathbb{Z}, \tag{3}$$

with $\mathbb{Z}$ denoting the space of integers. These integer constraints are rewritten to obtain the weighting coefficients

$$\alpha = \frac{i\lambda}{\lambda_1}, \qquad \beta = \frac{j\lambda}{\lambda_2}, \qquad \gamma = \frac{k\lambda}{\lambda_3}. \tag{4}$$

Mixed code-carrier combinations weight the phase part by τ and the code part by $1 - \tau$. The border cases are pure phase ($\tau = 1$) and pure code ($\tau = 0$) combinations. The parameter τ has a significant impact on the properties of the linear combination, and it is optimized later in this section. Replacing the weighting coefficients in $\tau = \alpha + \beta + \gamma$ by (4) yields the wavelength of the code-carrier combination

$$\lambda = \frac{\tau}{i/\lambda_1 + j/\lambda_2 + k/\lambda_3}. \tag{5}$$

The generalized widelane criterion is given for $\lambda_1 < \lambda_2 < \lambda_3$ by $\lambda > \lambda_3$. Equivalently, it can be expressed as a function of i, j, and k as

$$\tau > iq_{13} + jq_{23} + k > 0 \quad \text{with } q_{mn} = \frac{\lambda_n}{\lambda_m}. \tag{6}$$

The linear combination scales the ionospheric error by

$$A_I = \alpha + \beta q_{12}^2 + \gamma q_{13}^2 - a - bq_{12}^2 - cq_{13}^2. \tag{7}$$

The thermal noise of the elementary carrier phase measurements is assumed Gaussian with the standard deviation given by Kaplan and Hegarty [13]

$$\sigma_{\phi_i} = \frac{\lambda_i}{2\pi}\sqrt{\frac{B_L}{C/N_0}\left[1 + \frac{1}{2T \cdot C/N_0}\right]}, \tag{8}$$

where B_L denotes the loop bandwidth, C/N_0 the carrier-to-noise ratio, and T the predetection integration time. The overall noise contribution of the linear combination is

Table 1: Cramer-Rao bound for Galileo signals.

	Modulation	Bandwidth (MHz)	CRB (cm)
E1	BOC(1,1)	4	20
E5a	BPSK(10)	24	5
E5b	BPSK(10)	24	5
E5	BOC(15,10)	51	1

written as

$$N_m = \sqrt{(\alpha^2 + \beta^2 q_{12}^2 + \gamma^2 q_{13}^2) \cdot \sigma_{\phi_0}^2 + a^2\sigma_{\rho_1}^2 + b^2\sigma_{\rho_2}^2 + c^2\sigma_{\rho_3}^2} \tag{9}$$

with $\sigma_{\rho_1}^2, \ldots, \sigma_{\rho_3}^2$ being the noise variance of the code measurements. Table 1 shows the Cramer-Rao bound (CRB) for some Galileo signals as derived by Hein et al. [9]. A DLL bandwidth of 1 Hz has been assumed. The 4 MHz receiver bandwidth for E1 has been chosen to avoid sidelobe tracking.

For E1, E5a, E5b, E6 phase measurements, the wavelength scaling of σ_{ϕ_i} can be neglected due to the close vicinity of the frequency bands. However, it plays a major role when C-Band measurements are included.

Figure 2 shows the benefit of the code contribution to the $i = 1$ (E1), $j = -10$ (E5b), $k = 9$ (E5a) linear combination: a slight increase in noise level results in a considerable reduction of the ionospheric error. The phase weighting has been fixed to $\tau = 1$ so that α, β, γ, and λ are uniquely determined. The E5b and E5a code weights are adapted continuously and the ionosphere is eliminated in the border case

$$b = -c = \frac{\alpha + \beta q_{12}^2 + \gamma q_{13}^2}{q_{12}^2 - q_{13}^2}. \tag{10}$$

E1 code measurements have not been taken into account due to the increased noise level but might be included with a low weight.

The combination discrimination—measured by the ratio of half the wavelength and the noise level $\lambda/(2N_m)$—is proposed as a cost function to select linear combinations due to its independence of the geometry. It is shown for multiple ionosphere-free code-carrier combinations in Figure 3. The strong dependency on the phase weighting τ suggests an optimization with respect to this parameter. Note that the legend refers to the elementary wavelengths which have to be scaled by τ.

The computation of the optimum τ takes again only E5a/E5b code measurements into account as the benefit of the E1 code measurement is negligible ($a = 0$). The notation is simplified by

$$\begin{aligned} \lambda &= \widetilde{\lambda} \cdot \tau, \\ A_I &= \widetilde{\kappa} \cdot \tau - b q_{12}^2 - c q_{13}^2, \\ N_m &= \sqrt{\sigma_\phi^2 \cdot (\alpha^2 + \beta^2 q_{12}^2 + \gamma^2 q_{13}^2) + \sigma_\rho^2 \cdot (b^2 + c^2)} \\ &= \sqrt{\sigma_\phi^2 \cdot \widetilde{\eta}^2 \tau^2 + \sigma_\rho^2 \cdot (b^2 + c^2)}, \end{aligned} \tag{11}$$

with $\widetilde{\lambda}$, $\widetilde{\kappa}$, and $\widetilde{\eta}$ implicitly given by (5), (7), and (9). The

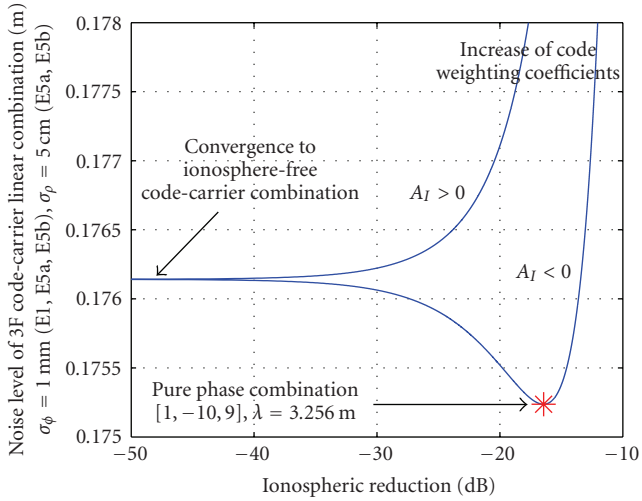

Figure 2: Adaptive code contribution to linear combinations: tradeoff between noise level and ionospheric reduction.

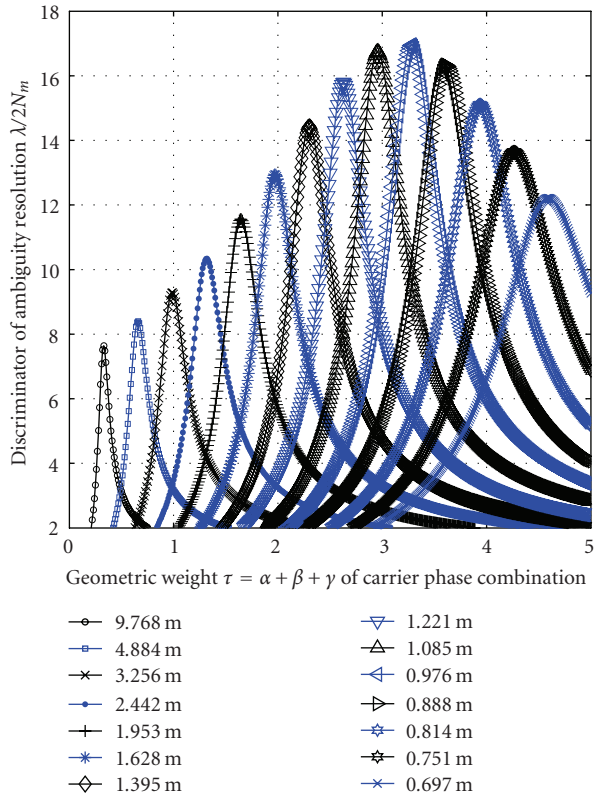

Figure 3: Optimal weighting of the phase combination part of ionosphere-free code-carrier combinations with $i = 1$, $k = -j - 1$, and $j \in \{-12, \ldots, 1\}$.

E5a/E5b code weights are determined from the ionosphere-free and geometry-preserving conditions as

$$\begin{aligned} b &= 1 - c - \tau, \\ c &= \underbrace{\frac{\widetilde{\kappa} + q_{12}^2}{q_{13}^2 - q_{12}^2}}_{w_1} \cdot \tau + \underbrace{\frac{-q_{12}^2}{q_{13}^2 - q_{12}^2}}_{w_2} = w_1 \cdot \tau + w_2. \end{aligned} \tag{12}$$

Table 2: Properties and weighting coefficients of ionosphere-free E1-E5b-E5a code-carrier combinations.

i	j	k	b	c	$\tilde{\lambda}$ (m)	λ (m)	N_m (m)	R
1	−12	11	0.327	0.344	9.768	3.217	0.28	5.81
1	−11	10	0.166	0.175	4.884	3.216	0.25	6.38
1	−10	9	0.006	0.007	3.256	3.214	0.23	7.05
1	−9	8	−0.154	−0.162	2.442	3.213	0.20	7.86
1	−8	7	−0.314	−0.330	1.954	3.212	0.18	8.84
1	−7	6	−0.474	−0.499	1.628	3.211	0.16	10.02
1	−6	5	−0.634	−0.667	1.396	3.210	0.14	11.42
1	−5	4	−0.793	−0.835	1.221	3.209	0.12	12.99
1	−4	3	−0.953	−1.003	1.085	3.208	0.11	14.54
1	−3	2	−1.112	−1.171	0.977	3.207	0.10	15.65
1	−2	1	−1.272	−1.339	0.888	3.206	0.10	15.85
1	−1	0	−1.431	−1.506	0.814	3.205	0.11	15.04
1	0	−1	−1.590	−1.674	0.751	3.204	0.12	13.59

The combination discrimination becomes from (5), (11), and (12):

$$R(\tau) = \frac{\lambda(\tau)/2}{N_m(\tau)} = \frac{\tilde{\lambda}\cdot\tau}{2\sqrt{\sigma_\phi^2\cdot\tilde{\eta}^2\tau^2+\sigma_\rho^2\cdot\left(\left(w_1\tau+w_2\right)^2+\left(1-\tau-w_1\tau-w_2\right)^2\right)}}. \quad (13)$$

Setting the derivative to zero yields the optimum weighting

$$\tau_{\text{opt}} = \frac{1-2w_2+2w_2^2}{1+w_1-w_2-2w_1w_2}, \quad (14)$$

which is independent of both σ_ρ and σ_ϕ. Table 2 contains the weighting coefficients and characteristics of the code-carrier combinations shown in Figure 3.

Figure 4 shows the benefit of adaptive code and phase weighting for the code-carrier linear combination with $i = 0$ (E1), $j = 1$ (E5b), and $k = -1$ (E5a). Obviously, the wavelength increases linearly with τ and the ionosphere can be eliminated with any τ. The noise amplification depends on the level of ionospheric reduction: a linear increase can be observed near the pure phase combination, while the increase becomes negligible for the ionosphere-free combination. Thus, the combination discrimination of the ionosphere-free code-carrier combination is increased by almost the same factor as τ is risen.

3. C-BAND AIDED CODE-CARRIER LINEAR COMBINATIONS

The 20 MHz wide C-Band (5010 · · · 5030 MHz = {489.736 · · · 491.691} · 10.23 MHz) has been reserved for Galileo. The higher frequency range has a multitude of advantages and drawbacks: an additional free space loss of 10 dB occurs which has to be compensated by a larger transmit power. The ionospheric delay is approximately 10 times lower than in the E1 band. The small wavelength of 5.9691 cm · · · 5.9839 cm complicates direct ambiguity resolution but results in an approximately 3.2 times lower standard deviation of phase noise. Moreover, the C-Band offers additional degrees of freedom for the design of linear combinations.

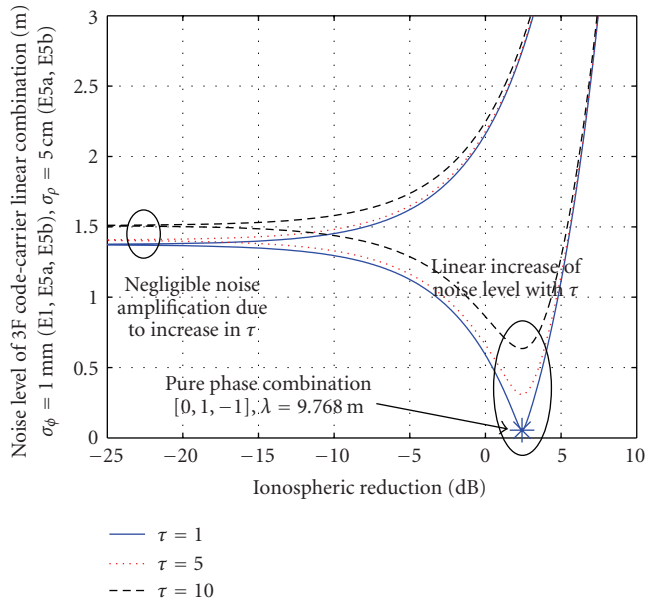

Figure 4: Benefit of adaptive code and phase weighting for linear combinations with $\lambda = \tau$ 9.768 m.

3.1. Reduced noise ionosphere-free code-only combinations

The design of three frequency code-only combinations that preserve geometry and eliminate ionospheric errors is characterized by one degree of freedom used for noise minimization. The weighting coefficients are derived from the geometry preserving and ionosphere-free constraints in (1), (7) as

$$a = 1-b-c,$$
$$b = \underbrace{-\frac{1}{q_{12}^2-1}}_{\nu_1} + \underbrace{\left(-\frac{q_{13}^2-1}{q_{12}^2-1}\right)}_{\nu_2}\cdot c = \nu_1+\nu_2\cdot c. \quad (15)$$

Minimization of $N_m^2 = a^2\sigma_{\rho_1}^2 + b^2\sigma_{\rho_2}^2 + c^2\sigma_{\rho_3}^2$ yields

$$c = \frac{(1-\nu_1+\nu_2-\nu_1\nu_2)\cdot\sigma_{\rho_1}^2 - \nu_1\nu_2\cdot\sigma_{\rho_2}^2}{(1+2\nu_2+\nu_2^2)\cdot\sigma_{\rho_1}^2 + \nu_2^2\cdot\sigma_{\rho_2}^2 + \sigma_{\rho_3}^2}. \quad (16)$$

Ionosphere-free code-only combinations with more than three frequencies are obtained by a multidimensional derivative. Table 3 shows that the pure L-band E1-E5b-E5a combination is characterized by a noise level of 44.41 cm. If the E5 signal is received with full bandwidth, the CRB is reduced to 1 cm but the number of degrees of freedom is reduced by one so that the noise level of the E1-E5 combinations are lightly

Table 3: Ionosphere-free code-only combinations with minimum noise $\sigma_\rho(\text{E1}) = \sigma_\rho(\text{C1}) = \cdots = \sigma_\rho(\text{C4}) = 20$ cm and $\sigma_\rho(\text{E5a, E5b}) = 5$ cm.

E1	E5b	E5a	C1	C2	C3	C4	N_m (cm)
2.090	1.500	−2.590	0	0	0	0	44.41
0.387	0.255	−0.506	0.863	0	0	0	19.14
0.213	0.128	−0.292	0.476	0.476	0	0	14.21
0.147	0.079	−0.211	0.328	0.328	0.329	0	11.80
0.112	0.054	−0.168	0.251	0.251	0.251	0.251	10.31

Table 4: Ionosphere-free code-only combinations with minimum noise $\sigma_\rho(\text{E1}) = \sigma_\rho(\text{C1}) = \cdots = \sigma_\rho(\text{C4}) = 20$ cm and $\sigma_\rho(\text{E5}) = 1$ cm.

E1	E5	C1	C2	C3	C4	N_m (cm)
2.338	−1.338	0	0	0	0	46.78
0.398	−0.278	0.879	0	0	0	19.31
0.217	−0.179	0.481	0.481	0	0	14.27
0.150	−0.142	0.331	0.331	0.331	0	11.84
0.114	−0.122	0.252	0.252	0.252	0.252	10.34

Table 5: Ionosphere-free code-carrier widelane combinations with $\sigma_\rho(\text{E1}) = \sigma_\rho(\text{C1}) = \cdots = \sigma_\rho(\text{C4}) = 20$ cm and $\sigma_\rho(\text{E5}) = 1$ cm.

i	j	k	l	m	n	a	b	λ	N_m
E1	E5	C1	C2	C3	C4	E1	E5	(m)	(cm)
1	−1	0	0	0	0	−4.4e−3	−3.11	3.21	3.92
1	−1	0	0	1	−1	−4.7e−3	−3.28	3.39	4.84
1	−1	0	1	−1	0	−4.7e−3	−3.28	3.39	4.84
1	−1	0	1	0	−1	−5.0e−3	−3.46	3.59	5.12
1	−1	1	−1	0	0	−4.7e−3	−3.28	3.39	4.84
1	−1	1	0	−1	0	−5.0e−3	−3.46	3.59	5.12
1	−1	1	0	0	−1	−5.3e−3	−3.67	3.81	5.43
0	0	−1	0	0	1	−8.5e−5	−6.0e−2	20.70	15.39

increased (Table 4). These combinations will play a role in conjunction with code-carrier combinations.

The C-band is split into 4 bands of 5 MHz bandwidth centered at $\{490, 490.5, 491, 491.5\} \cdot 10.23$ MHz and allows a significant reduction of the noise level. Note that the noise of any contributing elementary combination is reduced by a weighting coefficient smaller than one.

3.2. Joint L-/C-band widelane combinations

Code-carrier linear combinations can also include both L-band and C-band measurements. Therefore, (1)–(7) are extended to include the additional measurements. The weighting coefficients $\{\alpha, \beta, \gamma, \ldots\}$ and $\{a, b\}$ are computed such that the discriminator output of (13) is maximized for a given set of integer coefficients $\{i, j, k, \ldots\}$.

Table 5 contains ionosphere-free joint L-/C-band code-carrier widelane combinations ($\lambda > \max_i \lambda_i$). The E1-E5 pure L-band combination benefits from a noise level of only 3.92 cm which simplifies the resolution of the 3.215 m integer ambiguities. In contrast to the code-only combinations, the use of the full-bandwidth E5 signal is advantageous compared to separate E5a and E5b measurements. The C-band offers no benefit for these wavelengths. In the last row of Table 5, a linear combination with a pure L-band code and pure C-band phase part is described. The combination discrimination equals 67.25 but the noise level is also increased to 15.39 cm.

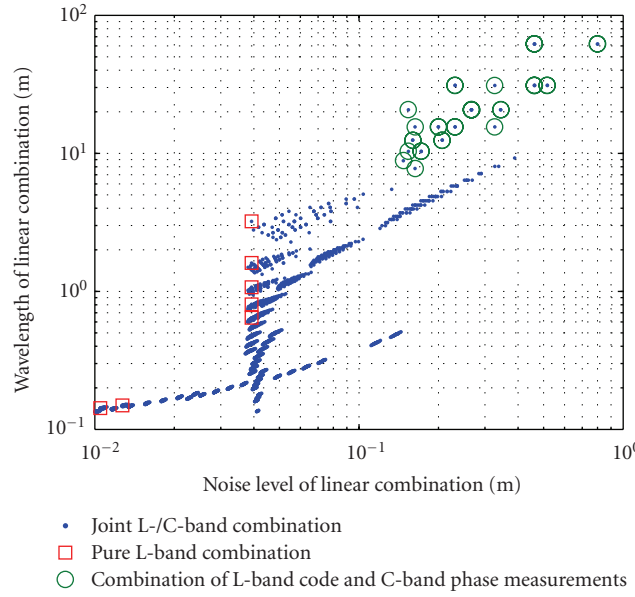

Figure 5: Comparison of joint L-/C-Band linear combinations for $\sigma_\rho(\text{E1}) = 20$ cm, $\sigma_\rho(\text{E5}) = 1$ cm and $\sigma_{\phi,i} = \lambda_i/\lambda_1 \cdot \sigma_{\phi_0}$ with $\sigma_{\phi_0} = 1$ mm.

Figure 5 shows the tradeoff between wavelength and noise level for joint L-/C-band ionosphere-free linear code-carrier combinations with $\{i, j\} \in [-5, +5]$ and $\{k, l, m, n\} \in [-2, +2]$. The E1-E5 combination is of special interest but the maximum combination discrimination is obtained for a joint L-/C-band combination.

3.3. Joint L-/C-band narrowlane combinations

There exists a large variety of joint code-carrier narrowlane combinations where C-band measurements help to reduce the noise substantially. Figure 6 shows the tradeoff between wavelength and noise level for $\{i, j\} \in [-5, +5]$ and $\{k, l, m, n\} \in [-2, +2]$. For $\lambda = 5.7$ cm, the consideration of C-band measurements reduces the noise level by a factor of 5 compared to a pure L-band combination (Table 6).

3.4. Reliability of ambiguity resolution

The integer ambiguity resolution is based on the linear combination of four different variable types: double-difference measurements for eliminating clock errors and satellite/receiver biases; multifrequency combinations for suppressing the ionosphere; code and carrier phase measurements for

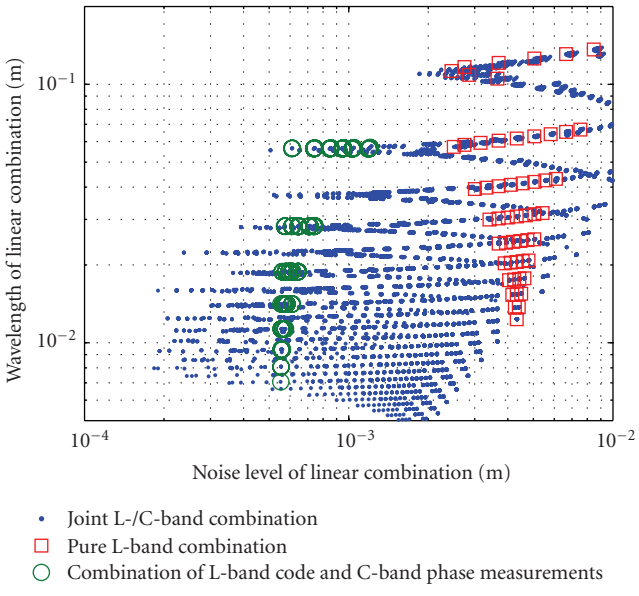

Figure 6: Comparison of joint L-/C-Band linear combinations for $\sigma_p(\mathrm{E1}) = 20\,\mathrm{cm}$, $\sigma_p(\mathrm{E5}) = 1\,\mathrm{cm}$ and $\sigma_{\phi,i} = \lambda_i/\lambda_1 \cdot \sigma_{\phi_0}$ with $\sigma_{\phi_0} = 1\,\mathrm{mm}$.

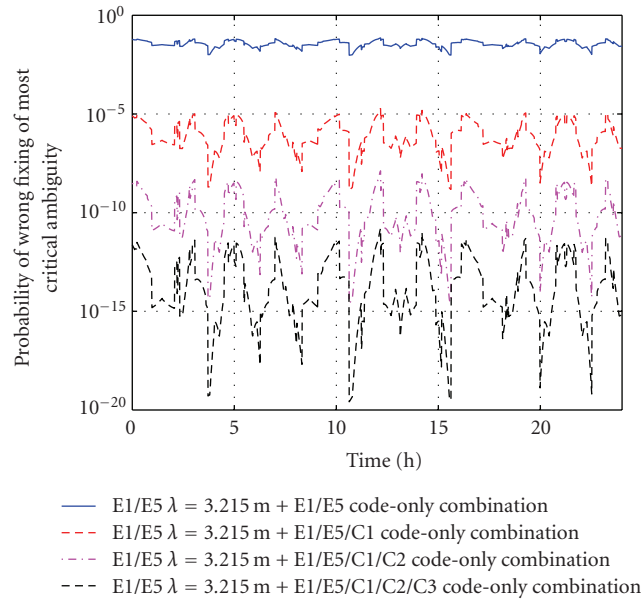

Figure 7: Reliability of $\lambda = 3.215\,\mathrm{m}$ integer ambiguity resolution: impact of C-band measurements on the probability of wrong fixing of the most critical ambiguity.

Table 6: Ionosphere-free code-carrier narrowlane combinations with $\sigma_p(\mathrm{E1}) = \sigma_p(\mathrm{C1}) = \cdots = \sigma_p(\mathrm{C4}) = 20\,\mathrm{cm}$ and $\sigma_p(\mathrm{E5}) = 1\,\mathrm{cm}$.

i	E1	1	0	−1	5
j	E5	−1	0	1	−3
k	C1	0	0	1	0
l	C2	0	0	0	0
m	C3	0	0	0	0
n	C4	1	1	0	0
a	E1	−2.04e−6	7.60e−5	1.58e−4	2.55e−4
b	E5	−1.43e−3	5.31e−2	0.110	0.178
λ	(cm)	5.55	5.65	5.76	5.73
N_m	(mm)	0.51	0.61	1.22	2.50
R		54.4	46.3	23.6	11.46

reducing the noise level; and finally, L-/C-band combinations for noise and discrimination characteristics.

Two joint L-/C-band code-carrier ionosphere-free combinations are chosen for real-time (single epoch) ambiguity resolution. The $\lambda = 3.215\,\mathrm{m}$, $N_m = 3.92\,\mathrm{cm}$ combination of Table 5 and one further combination of Table 4. The double difference (DD) ionosphere-free combinations are modeled as

$$\begin{bmatrix} y_{\rho\phi} \\ y_\rho \end{bmatrix} = \begin{bmatrix} G \\ G \end{bmatrix} \delta x + \begin{bmatrix} \lambda \cdot 1 \\ 0 \end{bmatrix} N + \varepsilon = X\beta + \varepsilon, \tag{17}$$

with

$$X = \begin{bmatrix} \lambda \cdot 1 & G \\ 0 & G \end{bmatrix}, \qquad \beta = \begin{bmatrix} N \\ \delta x \end{bmatrix} \tag{18}$$

and the DD geometry matrix G, the baseline δx and the integer ambiguities N. The double-differenced troposphere is assumed to be negligible or known a priori (e.g., from an accurate continued fraction model).

Note that the troposphere has the same impact on all geometry-preserving combinations and does not affect the optimization of the mixed code-carrier combinations. The noise vector is Gaussian distributed, that is,

$$\varepsilon \sim \mathcal{N}(0, \Sigma) \quad \text{with } \Sigma = \Sigma_{\mathrm{LC}} \otimes \Sigma_{\mathrm{DD}}, \tag{19}$$

where $\otimes$ denotes the Kronecker product. Σ_{LC} models the linear combination induced correlation and Σ_{DD} includes the correlation due to double difference measurements from N_s visible satellites. The standard deviation of the most critical ambiguity estimate can be written as

$$\sigma_{\max} = \max_{i=\{1\cdots N_s-1\}} \sqrt{\Sigma_{\hat{\beta}}(i,i)}, \quad \Sigma_{\hat{\beta}} = \left(X^T \Sigma^{-1} X\right)^{-1}, \tag{20}$$

and the probability of wrong fixing follows as

$$P_w^c = 1 - \int_{-0.5}^{+0.5} \frac{1}{\sqrt{2\pi\sigma_{\max}^2}} e^{-x^2/2\sigma_{\max}^2} dx. \tag{21}$$

In the following analysis, the location of the reference station is at 48.1507° N, 11.5690° E with a baseline length of 10 km.

Figure 7 shows the benefit of C-band measurements for integer ambiguity fixing. If the E1-E5 pure L-band combination is used as second combination in (17), the failure rate varies between 0.01 and 0.07 due to its poor noise characteristics. The use of two additional C-band measurements reduces the maximum probability of wrong fixing to 10^{-5}. For three C-band frequencies, the failure rate is at most 10^{-11}

which corresponds to a gain of 9 to 17 orders of magnitude compared to the pure L-band combination.

The reliability of ambiguity resolution can be further improved by using the LAMBDA method of Teunissen [7]. The float ambiguity estimates are decorrelated by an integer transformation Z^T and the ambiguity covariance matrix is written as

$$\Sigma_{\hat{N}'} = Z^T \Sigma_{\hat{N}} Z = LDL^T, \tag{22}$$

with the decomposition into a lower triangular matrix L and a diagonal matrix D. The probability of wrong fixing of the sequential bootstrapping estimator is given by Teunissen [14] as

$$P_w = 1 - \prod_{i=1}^{N_s-1} \int_{-0.5}^{+0.5} \frac{1}{\sqrt{2\pi\sigma_c^2(i)}} e^{-x^2/2\sigma_c^2(i)} dx, \tag{23}$$

with $\sigma_c(i) = \sqrt{D(i,i)}$. It represents a lower bound for the success rate of the integer least-square estimator and is depicted in Figure 8. Obviously, the use of joint L-/C-band linear combinations reduces the probability of wrong fixing by several orders of magnitude compared to pure L-band combinations.

3.5. Accuracy of baseline estimation

After integer ambiguity fixing, the baseline is re-estimated from (17). The covariance matrix of the baseline estimate in local coordinates is given by

$$\Sigma_{\delta\hat{x}} = R_L \left(G^T \Sigma^{-1} G\right)^{-1} R_L^T \tag{24}$$

with the rotation matrix R_L. Figure 9 shows the achievable horizontal and vertical accuracies for the two optimized joint L-/C-band combinations.

The pure L-band combinations in the first row of Tables 4 and 5 have been again selected as reference scenario. It can be observed that the use of joint L-/C-band linear combinations enables a slight improvement in position estimates compared to the significant benefit for ambiguity resolution.

4. JOINT L-/C-BAND CARRIER SMOOTHED CARRIER

Ionosphere-free code-carrier linear combinations are characterized by a noise level that is one to two orders of magnitude larger than of the underlying carrier-phase measurements (Table 5). Both noise and multipath of the code-carrier combinations can be reduced by the smoothing filter of Hatch [15] which is shown in Figure 10. The upper input can be an ionosphere-free code-carrier combination of arbitrary wavelength. The lower input is a pure ionosphere-free phase combination that is determined by three conditions: the first ensures that the geometry is preserved, the second eliminates the ionosphere, and the third minimizes the noise, that is,

$$\begin{aligned} &\alpha + \beta + \gamma \stackrel{!}{=} 1, \\ &\alpha + \beta q_{12}^2 + \gamma q_{13}^2 \stackrel{!}{=} 0, \\ &\min_{\alpha,\beta,\gamma} N_m^2 = \min_{\alpha,\beta,\gamma} \left(\sigma_{\phi,0}^2 \cdot (\alpha^2 + \beta^2 q_{12}^2 + \gamma^2 q_{13}^2)\right). \end{aligned} \tag{25}$$

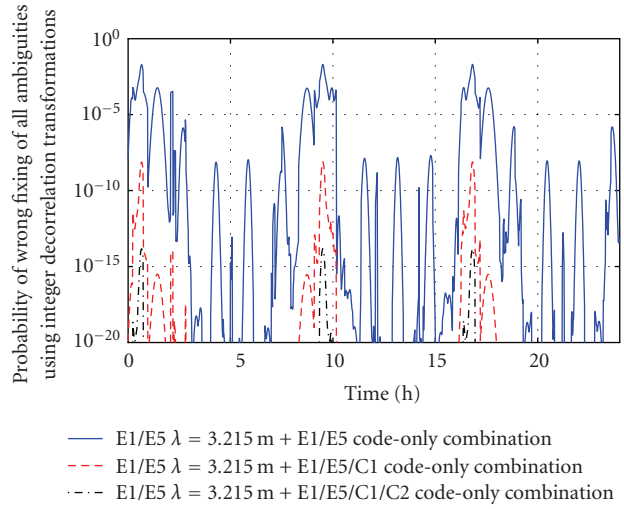

Figure 8: Reliability of $\lambda = 3.215$ m integer ambiguity resolution: impact of C-band measurements on the probability of wrong fixing based on sequential fixing with the integer decorrelation transformation.

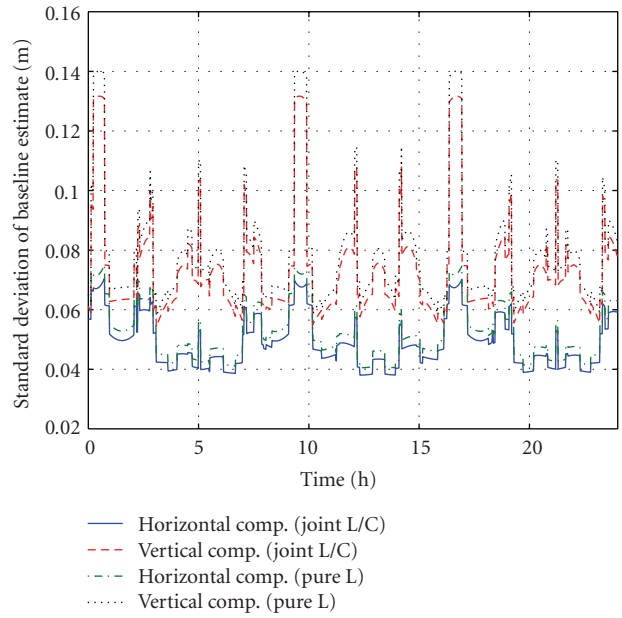

Figure 9: Standard deviation of baseline estimation using the $\lambda = 3.215$ m E1-E5 ionosphere-free code-carrier combination and the E1-E5-C1 · · · C4 ionosphere-free code-only combination.

Note that the superposition of ambiguities of the pure phase combination is not necessarily an integer number of a common wavelength. The respective ambiguities are not affected by the low pass filter and do not occur in the smoothed output $\lambda_A \overline{\phi}_A$ due to different signs in the addition to $\lambda_A \phi_A$ (Figure 10).

Table 7 shows an ionosphere-free E1-E5a-E5b phase combination that increases the noise level by a factor 2.64. However, the low noise level of C-band measurements suggests the use of the second combination with $f_3 = 491 \cdot 10.23$ MHz. In this case, the noise level is not only reduced

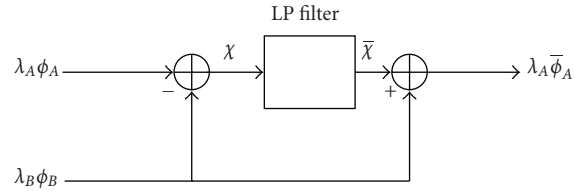

Figure 10: Ionosphere-free carrier smoothed code-carrier combinations.

Table 7: Weighting coefficients and properties of ionosphere-free carrier smoothed carrier phase combinations.

f_1	f_2	f_3	α	β	γ	N_m
E1	E5b	E5a	2.324	− 0.559	− 0.764	$2.64 \cdot \sigma_{\phi_0}$
E1	E5b	C	− 0.008	− 0.056	1.064	$0.34 \cdot \sigma_{\phi_0}$

by smoothing but also by the coefficients of the pure phase combination.

The variance of the smoothed combination is given by

$$\sigma_{\overline{A}}^2 = E\left\{\left(\overline{\varepsilon}_A(t) - \overline{\varepsilon}_B(t) + \varepsilon_B(t)\right)^2\right\}, \tag{26}$$

with the low-pass filtered noise (e.g., Konno et al. [16])

$$\overline{\varepsilon}_A(t) = \frac{1}{\tau_s} \cdot \sum_{n=0}^{\infty} \left(1 - \frac{1}{\tau_s}\right)^n \varepsilon_A(t-n), \tag{27}$$

and the smoothing time τ_s. Setting (27) into (26), and using the definition of a geometric series yields

$$\sigma_{\overline{A}}^2 = \sigma_B^2 + \frac{1}{2\tau_s - 1} \cdot \left(\sigma_A^2 + \sigma_B^2 - 2\sigma_{AB}^2\right) + \frac{2}{\tau_s} \cdot \left(\sigma_{AB}^2 - \sigma_B^2\right). \tag{28}$$

For long smoothing times, only the low noise of the joint L/C pure carrier-phase combination $\lambda_B\phi_B$ remains (Table 7).

5. CONCLUSIONS

In this paper, new joint L-/C-band linear combinations that include both code- and carrier-phase measurements have been determined. The weighting coefficients are selected such that the ratio between wavelength and noise level is maximized. An ionosphere-free L-band combination (IFL) could be found at a wavelength of 3.215 m with a noise level of 3.92 cm.

The combination of L- and C-band measurements reduces the noise level of ionosphere-free code-only combinations by a factor 4.5 compared to pure L-band combinations. This increases the reliability of an ambiguity resolution option for the IFL combination by 9 orders of magnitude.

The residual variance of the noise can be further reduced by smoothing. An L-/C-band carrier combination can smooth the noise with a residual variance below the L-band phase noise variance. The smoothed solution can either be used directly or can be used to resolve the narrowlane ambiguities. The variance is basically the same in both cases. The resolved ambiguities, however, provide instantaneous independent solutions.

REFERENCES

[1] B. Forssell, M. Martin-Neira, and R. A. Harris, "Carrier phase ambiguity resolution in GNSS-2," in *Proceedings of the 10th International Technical Meeting of the Satellite Division of the Institute of Navigation (ION GPS '97)*, vol. 2, pp. 1727–1736, Kansas City, Mo, USA, September 1997.

[2] J. Jung, P. Enge, and B. Pervan, "Optimization of cascade integer resolution with three civil frequencies," in *Proceedings of the 13th International Technical Meeting of the Satellite Division of the Institute of Navigation (ION GPS '00)*, Salt Lake City, Utah, USA, September 2000.

[3] M. Cocard and A. Geiger, "Systematic search for all possible Widelanes," in *Proceedings of the 6th International Geodetic Symposium on Satellite Positioning*, Columbus, Ohio, USA, March 1992.

[4] P. Collins, "An overview of gps inter-frequency carrier phase combinations," Technical Memorandum, Geodetic Survey Division, University of New Brunswick, Ottawa, Ontario, Canada, 1999.

[5] P. Henkel and C. Günther, "Three frequency linear combinations for Galileo," in *Proceedings of the 4th Workshop on Positioning, Navigation and Communication (WPNC '07)*, pp. 239–245, Hannover, Germany, March 2007.

[6] P. Henkel and C. Günther, "Sets of robust full-rank linear combinations for wide-area differential ambiguity fixing," in *Proceedings of the 2nd ESA Workshop on GNSS Signals and Signal Processing*, Noordwijk, The Netherlands, April 2007.

[7] P. Teunissen, "Least-squares estimation of the integer ambiguities," Invited lecture, Section IV, Theory and Methodology, IAG General Meeting, Beijing, China, 1993.

[8] P. J. G. Teunissen, "On the GPS widelane and its decorrelating property," *Journal of Geodesy*, vol. 71, no. 9, pp. 577–587, 1997.

[9] G. Hein, J. Godet, J. Issler, et al., "Status of galileo frequency and signal design," in *Proceedings of the 15th International Technical Meeting of the Satellite Division of the Institute of Navigation (ION GPS '02)*, pp. 266–277, Portland, Ore, USA, September 2002.

[10] "Galileo Open Service Signal-in-Space ICD," http://www.galileoju.com.

[11] European Radiocommunications Office, "The European Table of Frequency Allocations and Utilisations in the Frequency Range 9 kHz to 1000 GHz," ERC Report 25, p. 132, 2007.

[12] M. Irsigler, G. Hein, B. Eissfeller, et al., "Aspects of C-band satellite navigation: signal propagation and satellite signal tracking," in *Proceedings of the European Navigation Conference (ENC GNSS '02)*, Kopenhagen, Denmark, May 2002.

[13] E. Kaplan and C. Hegarty, *Understanding GPS: Principles and Applications*, Artech House, London, UK, 2nd edition, 2006.

[14] P. J. G. Teunissen, "Success probability of integer GPS ambiguity rounding and bootstrapping," *Journal of Geodesy*, vol. 72, no. 10, pp. 606–612, 1998.

[15] R. R. Hatch, "A new three-frequency, geometry-free, technique for ambiguity resolution," in *Proceedings of the 19th International Technical Meeting of the Satellite Division of the Institute of Navigation (ION GNSS '06)*, vol. 1, pp. 309–316, Fort Worth, Tex, USA, September 2006.

[16] H. Konno, S. Pullen, J. Rife, and P. Enge, "Evaluation of two types of dual-frequency differential GPS techniques under anomalous ionosphere conditions," in *Proceedings of the National Technical Meeting of the Institute of Navigation (NTM '06)*, vol. 2, pp. 735–747, Monterey, Calif, USA, January 2006.